

The nature of frequency-angular diffusion of powerful quiresonant radiation

A. I. Plekhanov, S. G. Rautian, V. P. Safonov, and B. M. Chernobrod

Institute of Automation and Electrometry, Siberian Branch of the Academy of Sciences of the USSR, Novosibirsk

(Submitted 28 July 1984)

Zh. Eksp. Teor. Fiz. **88**, 426–435 (February 1985)

An experimental study has been carried out of radiation emitted in $3S_{1/2}-3P_{3/2}$ transitions under quiresonant excitation of sodium vapor. It was shown that conical radiation appeared as a result of four-photon parametric scattering of self-focused exciting radiation, with three interacting waves propagating in the same direction. The angle at which the conical radiation was observed was not then equal to the phase-matching angle for plane waves, but the condition for spatial phase-matching with respect to the longitudinal coordinate was satisfied. This interpretation is confirmed by experiments with bichromatic excitation.

1. INTRODUCTION

There have been numerous studies of the frequency-angular diffusion of powerful quiresonant radiation in gases (see Ref. 1 for bibliography). Conical radiation, emitted when the frequency of the powerful radiation is greater than the frequency of the absorption line, has attracted particular attention. The transverse far-field distribution of the transmitted radiation takes then the shape of a ring (Fig. 1a) coaxial with the incident beam. The spectrum of the conical radiation is shifted toward low frequencies relative to the resonance line, and corresponds to the scattering branch lying in the top left corner of Fig. 1b.¹⁾ This branch was first observed in Ref. 2 and was interpreted as the result of four-photon parametric luminescence in which two strong-field photons (ω_L, \mathbf{k}_L) generate two luminescence photons $(\omega_P, \mathbf{k}_P; \omega_3, \mathbf{k}_3)$. The frequencies and scattering angles were related in Ref. 2 by the following phase-matching condition for plane waves:

$$2\mathbf{k}_L = \mathbf{k}_3 + \mathbf{k}_P, \quad 2\omega_L = \omega_3 + \omega_P, \quad |\mathbf{k}_i| = n_i(\omega_i) \omega_i / c. \quad (1)$$

According to condition (1), waves with vectors \mathbf{k}_P and \mathbf{k}_3 should be deflected in opposite directions through equal angles from the direction of \mathbf{k}_L . Subsequent experiments have clearly shown that only the ω_P radiation is so deflected whereas radiation near ω_3 propagates along \mathbf{k}_L . This has led to many new hypotheses on the origin of the conical radiation, but none is in agreement with experimental data.¹⁾

It is, however, important to note that there are specific conditions under which conical radiation is observed: the onset of conical emission is correlated with the development of small-scale self-focusing,³⁻⁶ and experiments have shown that the emission at the frequency of the three-photon line arises near the entrance window of the cell, and is then amplified during propagation within the scattering volume. Both the laser field (ω_L) and the radiation at the frequency ω_3 are then localized in the self-focusing filaments. The parametric interaction between the above waves is also found to induce nonlinear polarization at the frequency $\omega_P = 2\omega_L - \omega_3$.

Localization of the four-photon parametric process in a filament of small cross section leads to a change in the direction of the interference maximum⁷ and scattering occurs

without conservation of the transverse momentum components, but the spatial phase-matching conditions are satisfied for the longitudinal coordinate:

$$2k_L = k_3 + k_P \cos \theta, \quad 2\omega_L = \omega_3 + \omega_P. \quad (2)$$

This situation is totally analogous to that examined in the theory of stimulated Raman scattering of anti-Stokes and higher Stokes components in focused beams. This theory is discussed in Refs. 8–10, where it is shown that the spectral components of scattered radiation have intensity maxima at angles to the axis that do not satisfy the spatial phase-matching conditions (1). According to Refs. 8 and 9, the angles of scattering may vary from the usual values corresponding to (1) to values exceeding those predicted by (1) by a factor of two, depending on the beam geometry of the interacting waves. The results reported in Refs. 8 and 9 may be used as a basis for showing that, in the interaction of self-focused Gaussian beams at frequencies ω_L and ω_3 , the scattering angle at frequency ω_P will be close to the Cerenkov values [see Eq. (7) below].

The assumption that conical radiation is the result of four-photon resonant parametric scattering in filaments of small cross section can be verified by the probing-field method in which the medium is illuminated by a bichromatic field in which the frequency of the second component ω_μ lies in the region of the three-photon line ω_3 (or in the region of ω_P), and the directions of propagation of the strong and probing fields are the same. In view of the foregoing ideas, conical radiation should arise³ at the frequency $\omega'_\mu = 2\omega_L - \omega_\mu$ that is symmetric in ω_μ relative to ω_L , and at an angle close to the value predicted by (2).

This paper presents the result of a detailed experimental study of conical radiation in sodium vapor. The probing-field method was used to show that this radiation was due to four-photon parametric scattering of the form described by (2).

2. BASIC RELATIONSHIPS

Consider four-photon parametric interactions when the exciting wave ω_L and the wave ω_3 are focused. Following Ref. 8, the complex amplitude of the field $E_P(\mathbf{r})$ at frequency ω_P will be written in the form

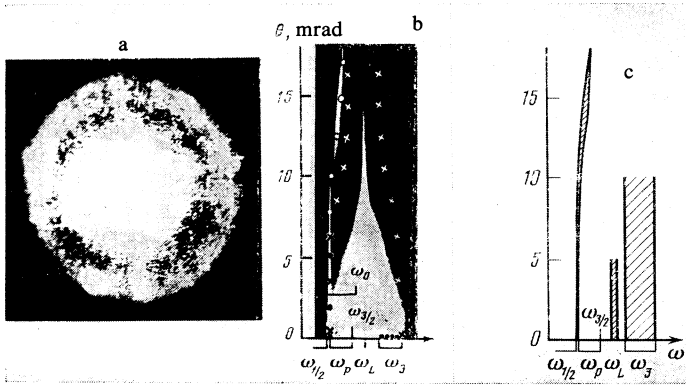


FIG. 1. a—Far-field intensity distribution of scattered radiation on the transverse plane; b—frequency-angular diagram of scattered radiation $\Omega_{3/2} = 9.9 \text{ cm}^{-1}$, $N = 3.7 \times 10^{14} \text{ cm}^{-3}$, $J_L = 0.3 \text{ mW/cm}^2$, calculation based on (9) with $K = 1.0$ (crosses) and $K = 1.41$ (points); c—calculated frequency angular diagram based on (2) for the same parameters as in diagram b but including $\Delta\omega_L = 4 \text{ cm}^{-1}$.

$$E_P^*(\mathbf{r}) = \frac{\alpha_P \exp(ik_P r)}{4\pi r} \int_V dr E_3^* E_L^2 \exp(-ik_P \mathbf{nr}), \quad (3)$$

where E_L and E_3 are the complex field amplitudes at frequencies ω_L and ω_3 , α_P is a parameter that depends on the cubic susceptibility at frequencies ω_P , and $n = \mathbf{r}/r$. In the case of Gaussian beams that are equally focused along the z axis, we have⁸

$$E_{L,3} = \frac{\tilde{\epsilon}_{L,3}}{1+iz/l_0} \exp\left(ik_{L,3}z - \frac{1}{2a_0^2} \frac{1}{1+iz/l_0} r_{\perp}^2\right), \quad (4)$$

where $\tilde{\epsilon}_{L,3}$ are the complex field amplitudes at $z = 0$ on the beam axis, and a_0 and l_0 are, respectively, the radius of the focal region and the diffractive divergence length of the beams under consideration. It is assumed that the beams have the minimum radius at the point $z = 0$, $r_1^2 = x^2 + y^2$. We then have⁸

$$E_P^*(\mathbf{r}) = -\frac{\alpha_P \exp(ik_P r)}{4r} \int_0^l dz \frac{\tilde{\epsilon}_3^* \tilde{\epsilon}_L^2 \beta_P(z)}{\gamma_P(z)} \exp[i\Phi(z)], \quad (5)$$

where

$$\begin{aligned} \beta_P(z) &= \frac{1}{[1+(z/l_0)^2](1+iz/l_0)}, \\ \gamma_P(z) &= -\frac{1}{a_0^2(1+iz/l_0)} - \frac{1}{2a_0^2(1-iz/l_0)}, \\ \Phi(z) &= \left(\frac{1}{2}k_P\theta^2 - \Delta k\right)z - i\frac{k_P^2\theta^2}{4\gamma_P(z)}, \\ n_z &= 1 - \frac{\theta^2}{2}, \quad \theta^2 = n_x^2 + n_y^2, \end{aligned}$$

$\Delta k = k_3 + k_P - 2k_L$, and l is the length of the medium.

When $z/l_0 \lesssim 1$, the intensity maximum at frequency ω_P occurs at the angle corresponding to $d[\text{Re}\Phi(z)]/dz = 0$:

$$\theta = \left\{ 2\Delta k/k_P \left[1 - \frac{k_P a_0^2}{l_0} \frac{9+26(z/l_0)^2+(z/l_0)^4}{[9+(z/l_0)^2]^2} \right] \right\}^{1/2}. \quad (6)$$

For Gaussian beams in a homogeneous linear medium, we have $l_0 = k_i a_0^2$. The neck of the beam becomes elongated in a nonlinear medium, as in our case^{8,11} ($l_0 \gg k_i a_0^2$). When this fact is taken into account in (6), and if we suppose that the frequencies $\omega_L, \omega_3, \omega_P$ are not very different, we obtain the Čerenkov angle

$$\theta_c \approx [2(n_3 + n_P - 2n_L)]^{1/2}. \quad (7)$$

The same angle is obtained from (2). The angular width of the radiation scattered at the Čerenkov angle is

$$\delta\theta_c \approx \pi(k_P l \theta_c)^{-1}. \quad (8)$$

The expression given by (7) describes the shape of the four-photon resonant parametric scattering branch.

The degree of agreement between experimental and calculated scattering branches is measured by the ratio K of the scattering angle and the square root of the difference between the refractive indices at the frequencies of the interacting waves. When $K = 1.41$, the formula

$$\theta = K(n_3 + n_P - 2n_L)^{1/2} \quad (9)$$

gives the scattering angles that follow from (2), whereas for $K = 1.0$ it gives the angles that follow from (1). When the frequency ω_i is close to the D -lines, the refractive index is given by

$$n_i \approx n(\omega_i) = 1 + \frac{\pi N e^2}{m \omega_i} \left(\frac{f_{3/2}}{\omega_{3/2} - \omega_i} + \frac{f_{1/2}}{\omega_{1/2} - \omega_i} \right), \quad (10)$$

where N is the concentration of the sodium atoms and $\omega_{3/2}, f_{3/2}$ and $\omega_{1/2}, f_{1/2}$ are the frequencies and oscillator strengths of the $3S_{1/2} - 3P_{3/2}$ and $3S_{1/2} - 3P_{1/2}$ transitions, respectively.

3. EXPERIMENTAL SETUP AND PROCEDURE

The experimental data presented below were obtained with a pulsed dye laser (PDL).¹² The peak PDL power was 1 kW, the pulse length was 5 ns, the divergence was 2.5 mrad, and the spectral width was either 0.02 or 0.2 cm^{-1} . The PDL frequency could be tuned near the D -lines of the sodium atom. The PDL wavelength was calibrated to within 0.1 Å (0.3 cm^{-1}), whereas relative changes could be determined to within 0.03 Å (0.1 cm^{-1}). The PDL enabled us to produce bichromatic radiation in which the frequency difference between the spectral components and their intensity could be varied. Monochromatic illumination was achieved by introducing a preliminary monochromator that removed the wide-band luminescence due to the dye. This preliminary monochromator was placed between the PDL and the cell containing the vapor.

The PDL radiation was focused in a cell (length $l = 20$

cm) containing sodium vapor at a density of 10^{13} – 10^{15} cm^{-3} . The temperature of the cell wall could be measured to within 2° . Radiation leaving the cell was focused onto the entrance slit of the SDL-1 diffraction spectrometer (linear dispersion $46 \text{ cm}^{-1}/\text{mm}$, with gratings were stopped down so that the relative aperture of the system was 1:10). The slit was located in the focal plane of a condenser lens ($f = 250 \text{ mm}$). This arrangement produced the angular (along the height of the slit image) and frequency distribution in the plane of the 2-mm wide exit slit. The spectrograms were recorded on photographic film and control measurements showed that a spectral resolution of 0.6 cm^{-1} was achieved on the spectrograms for an angular resolution of 0.1 mrad. The energy characteristics of the scattered radiation were measured by a photomultiplier and an oscillograph at a narrow exit slit of the spectrometer.

The intensity distributions at frequencies $\omega_L, \omega_3, \omega_P$ in sections running along the length of the cell, were examined using an optical system consisting of two objectives and a narrow-band filter. The latter was a Fabry-Perot interferometer located in a pressurized chamber. The magnified image of the beam cross section was recorded on photographic film. When the beam cross section at frequency ω_P was examined, an opaque disk was placed in the focal plane of the objective nearer the cell in order to cut off the powerful exciting radiation. The optical system that we have employed enabled us to observe beam inhomogeneities of the order of 10 – $20 \mu\text{m}$.

4. EXPERIMENTAL RESULTS

Conical radiation was found to leave the medium (Fig. 1a) for detunings $\Omega_{3/2} = \omega_L - \omega_{3/2}$ less than 20 cm^{-1} and exciting power densities $J_L \sim 0.3 \text{ MW}/\text{cm}^2$. For exciting power density $J_L \sim 0.1 \text{ MW}/\text{cm}^2$, the minimum sodium vapor density N and the maximum detuning necessary for the observation of conical radiation were related by $\Omega_{3/2}^3/n = 70 \pm 10 \text{ cm}^{-3}$, where $\Omega_{3/2}$ is in cm^{-1} and $n = N \times 10^{-14} \text{ cm}^{-3}$ is a dimensionless quantity.

Let us first consider the measured conical radiation as a function of exciting power. We found the aperture of the scattered cone near the frequency $\omega_{3/2}$ was independent of J_L . The conical-radiation power depends on the laser output power as follows: $P_P \propto P_L^{1.8 \pm 0.2}$. The dependence of the conical radiation intensity on the laser intensity is thus nearly quadratic, and for linear amplification this may be interpreted as an indication of its four-photon origin. The maximum radiation power in the ring was approximately 1% of the laser power.

We now turn to an analysis of the frequency-angular diagram of the scattered radiation. As noted above, the spectrogram of the observed radiation consists of the scattered branch ω_P and the broadened laser spectrum (see Fig. 1b). In the long-wave region, the scattered branch degenerates to a narrow spectral line at zero angle near the absorption line $\omega_{1/2}$ (Fig. 1b). As the detuning $\Omega_{3/2}$ is varied, the zero-angle line (ω_0) shifts in accordance with the calculation based on the phase-matching condition for four-photon resonant parametric scattering (solid line in Fig. 2). The quantity Ω_P in

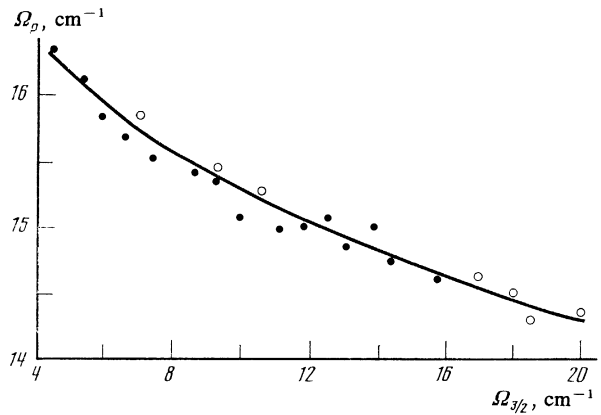


FIG. 2. Position of the zero-angle line relative to the frequency of the $3S_{1/2}$ – $3P_{3/2}$ resonant transition as a function of detuning $\Omega_{3/2}$: ●— $3.7 \cdot 10^{14} \text{ cm}^{-3}$; ○— $(9-11) \cdot 10^{14} \text{ cm}^{-3}$.

Fig. 2 stands for $\Omega_P = \omega_{3/2} - \omega_0$. As the vapor density N is varied, the position of the zero-angle line remains the same, which is again in agreement with the four-photon nature of the scattering process.

The spectrogram of Fig. 1b shows calculations based on (9) with $K = 1.0$ and $K = 1.41$ for the four-photon resonant parametric scattering process. The scattering branch, calculated for plane waves ($K = 1.0$), is always found to lie below the observed branch. This type of check was carried out for a wide range of concentrations N (10^{13} – 10^{15} cm^{-3}) and detuning $\Omega_{3/2}$ (2 – 20 cm^{-1}). Equation (9) was always confirmed for $K = 1.41$. We note that the spread in the measured temperatures ($\Delta T = 2^\circ \text{C}$) ensured an 8% precision in N , i.e., the angles were calculated to within 4%.

Our experiments gave us θ^2 as a function of N for $\Omega_{3/2} = 6 \text{ cm}^{-1}$, where θ is the angle at which the scattered branch can be seen at distances $\Omega_P = \omega_{3/2} - \omega_P = 2.5 \text{ cm}^{-1}$, 5 cm^{-1} , and 7.5 cm^{-1} (toward lower frequencies) from the absorption line $\omega_{3/2}$. For each point, the dependence of θ^2 on N could be satisfactorily approximated by a straight line $y = ax + d$. The coefficients a and d were determined by the least-squares method for each detuning, and their values are listed below (second column). The third column lists the values based on (7) and (10). The coefficient a calculated for plane waves is lower by a factor of two.

$\Omega_P, \text{ cm}^{-1}$	$\theta^2_{\text{exp}}, \text{ mrad}^2$	$\theta_r^2, \text{ mrad}^2$
2.5	$(99 \pm 12)n + (16 \pm 16)$	$115n$
5	$(67 \pm 3)n + (16 \pm 4)$	$80n$
7.5	$(51 \pm 3)n + (18 \pm 7)$	$68n$

The values of the coefficients in the interpolation functions are thus seen to be closer to those calculated from (7). We note that (7) does not take into account the effect of the divergence of the exciting radiation on the scattering angles. The true scattering angle is given by $\theta^2 = \theta_r^2 + \theta_L^2$. The values of the coefficient d in the interpolation lines are therefore the squares of the laser divergence angles due to the self-focusing effect, and are in satisfactory agreement with measurements.

As noted before, one of the conditions for the appearance of conical radiation under the conditions of partial

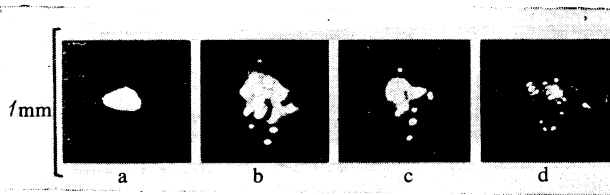


FIG. 3. Cross section of beams inside the cell for different frequencies ($\Omega_{3/2} = 4 \text{ cm}^{-1}$, $N = 10^{14} \text{ cm}^{-3}$, $J_L = 0.3 \text{ MW/cm}^2$): a— ω_L (cold cell); b— ω_L ; c— ω_3 ; d— ω_P .

phase-matching (2) is that the lateral dimensions of the scattering volumes must be small. It is therefore important to know the transverse intensity distribution of the interacting waves within the cell containing the sodium vapor (Fig. 3). We found that, when the conical radiation appeared, the exciting light beam of frequency ω_L split into several fine spots, i.e., we observed self-focusing (Fig. 3b). When the power and vapor density are increased, the number of spots increases with decreasing detuning, and the spot diameter falls to approximately $50 \mu\text{m}$. The intensity within the spots becomes greater than the intensity in the beam by a factor of 1.5–2, but their total area is, on average, 4–5 times smaller than the beam area. The spots thus contain about one-half to one-third of the total incident power.

Photography of the beam structure at frequency ω_3 (Fig. 3c) reveals that it is analogous to the structure of the incident beam, and that the analogy persists as the radiation propagates along the cell. Radiation of frequency ω_3 appears within the first few centimeters in the medium, and propagates with increasing intensity along the cell. The power within the spots at frequency ω_3 accounts for less than half the total power at this frequency, and most of the radiation propagates within the original total aperture of the pump beam. We find that, when the radiation is divided between the frequencies ω_3 and ω_L , radiation of frequency ω_P appears within the filament. This radiation is also found to propagate in narrow filaments (Fig. 3d). The spot diameters at frequency ω_P decreases as the beam propagates along the cell, reaching approximately $20 \mu\text{m}$ at exit from the medium. The onset of conical radiation is thus clearly correlated with the onset of self-focusing, and the four-photon parametric process $\omega_P = 2\omega_L - \omega_3$ develops in the multifilamentary structure of the self-focused laser beam.

The onset of self-focusing should lead to an increase in the diffractive divergence of the radiation of frequency ω_3 . Photoelectric measurements have shown that the fraction of this radiation at angles exceeding 12 mrad amounts to about 10^{-3} of the intensity integrated over the angles. The estimated relative intensity of the diffraction wings, based on the assumption of near-Gaussian intensity distribution within the multifilamentary structure of the self-focused beam,¹¹ yields 3×10^{-4} for self-focused spot diameters of $50 \mu\text{m}$ and angles exceeding 12 mrad, which is in complete agreement with the measured value. These low-intensity wings of the spectral components of the ω_3 radiation are not seen in the spectrograms of Fig. 1b, and the asymmetry of the frequency-angular diagrams is quite clear.

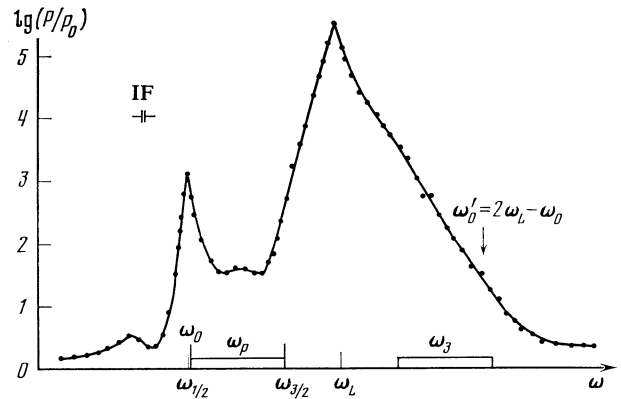


FIG. 4. Transmitted line profile ($\Omega_{3/2} = 10 \text{ cm}^{-1}$, $N = 3 \times 10^{14} \text{ cm}^{-3}$, monochromator slit $10 \mu\text{m}$; P_0 —minimum signal, IF—instrumental function of monochromator).

We paid particular attention to verification of the Manley-Rowe relations during the generation of the conical radiation. Since this question has frequently been raised in discussions, let us examine it in greater detail. The law of conservation of energy must be satisfied in this case for the radiation integrated over the angles and spectral intervals within which phase-matching is satisfied. Figure 4 shows the line profile integrated with respect to the angles, as it appears past the cell containing the sodium vapor. The profile was recorded photometrically. In Fig. 4, the conical radiation corresponds to the broad maximum in the region of ω_P and the zero-angle line corresponds to the narrow peak at ω_0 . It is clear from Fig. 4 that the power at the frequencies of the conical radiation is close to the power in the spectral components $\omega_3 = 2\omega_L - \omega_P$ symmetric to it. At the same time, the spectral power $P(\omega_0)$ in the zero-angle line is appreciably greater than the spectral power $P(\omega'_0)$ at frequency $\omega'_0 = 2\omega_L - \omega_0$.

However, it is important to recall two important factors. Firstly, Fig. 4 demonstrates the considerable broadening of the spectrum of exciting radiation as it propagates through the sodium vapor. While the laser-spectrum width at the 0.01 level of peak value in the frequency distribution $P(\omega_L)$ does not exceed 2 cm^{-1} at entry to the cell, the corresponding figure at exit from the cell is as high as 20 cm^{-1} . Secondly, the different spectral components of laser radiation broadened by propagation in sodium vapor contribute to excitation in the parametric interaction $2\omega_L = \omega_0 + \omega_3$, and give rise to the narrow zero-angle line of width $\Delta\omega_0 \approx 1 \text{ cm}^{-1}$. Actually, the plot in Fig. 2 shows that when ω_L changes by 14 cm^{-1} the frequency ω_0 shifts by only 1.7 cm^{-1} . Special measurements have shown that laser components from a region of width $\Delta\omega_L \approx 4 \text{ cm}^{-1}$ provide a strong-field contribution to the four-photon resonant parametric scattering process. The high-frequency radiation interacting with ω_L and ω_0 then fills a spectral band of width $\Delta\omega = 2\Delta\omega_L + \Delta\omega_0 \approx 9 \text{ cm}^{-1}$. Comparison of powers integrated over the intervals $\Delta\omega_0$ and $\Delta\omega$ shows that the integrated power within the ω_0 line is greater by a factor of 3–4 than the integrated power within the higher-frequency com-

ponent. The spectral properties of ω_0 are thus seen to correspond to the four-photon resonant parametric scattering process, whereas the situation in relation to the energy characteristics is not completely clear.

The fact that the exciting radiation is not monochromatic must also influence the part of the scattering branch that corresponds to conical radiation. Figure 1c shows the frequency-angular diagram calculated for exciting radiation with a spectrum 4 cm^{-1} wide. Comparison of Figs. 1c and b shows that there is good agreement between the calculated and experimental shape of the scattered branch. Broadening of exciting radiation leads to some (up to 10%) angular diffusion of the ω_p branch.

5. EXPERIMENTS WITH A PROBING FIELD

A direct verification of whether or not conical radiation is due to a four-photon interaction of the form described by (2) can be performed by the probing-field method in which the medium is exposed to a strong field and, at the same time, to a weak field propagating in the same direction with frequency ω_μ close to the frequency of the three-photon line. If the probing-field frequency lies in the region of parametric amplification, the presence of this field gives rise to a four-photon resonant parametric scattering process of the form $2\omega_L \rightarrow \omega_\mu + \omega'_\mu$. An intensity maximum at $\omega'_\mu = 2\omega_L - \omega_\mu$, which is the mirror image of ω_μ in ω_L , should then occur in the region of the scattering branch. The frequencies ω_μ, ω'_μ and angles θ between the waves $\mathbf{k}_\mu \parallel \mathbf{k}_L$ and \mathbf{k}'_μ for which the phase-matching interaction occurs for given frequency ω_L are then related by (7).

Figure 5a shows the spectrogram for bichromatic excitation. As can be seen, the introduction of the probing field leads to the appearance of a maximum in scattering. This maximum is symmetric to the probing field frequency relative to the laser frequency, and the scattering angle is equal to the angle in the absence of the probing field and corresponds to $K \approx 1.4$. When the probing field is retuned in the region of ω_3 , the intensity maximum on the frequency-angular diagram changes its position both in angle and frequency. Its position on the frequency scale was specified by $\omega'_\mu = 2\omega_L - \omega_\mu$, and the angle was set approximately by $K \approx 1.41$. Conical radiation of frequency ω'_μ occurred only

when the probing field lay on the high-frequency side of the three-photon line ($\omega_{3\text{ph}}^{3/2} = 2\omega_L - \omega_{3/2}$). This fact is in agreement with the four-photon parametric interaction since, for $\omega_\mu < \omega_{3\text{ph}}^{3/2}$, the difference between the refractive indices at the frequencies of the interacting waves is less than zero and (9) shows that conical scattering is impossible.

As already noted, the similarity between the probing-field method and the original spontaneous creation of photons with frequencies ω_p and ω_3 lies in the fact that, in both cases, the directions of the two waves are given, i.e., they are the waves with frequencies ω_μ and ω_L in the first case and ω_3 and ω_L in the second. The probing-field method produces conical radiation of frequency $\omega'_\mu = 2\omega_L - \omega_\mu$ when the probing-field frequency falls into the region of the ω_p branch. The spectrogram of Fig. 5b shows an example of this scattering. Four-photon resonant parametric scattering produces a maximum at an angle set by the ratio $K \approx 1.4$; this is in agreement with the Čerenkov value ($K \approx 1.41$).

When the frequency of the probing field falls into the interval $\Delta\omega_0$ on the ω_p branch, scattered radiation of frequency $\omega'_\mu = 2\omega_L - \omega_\mu$ that is symmetric relative to the laser frequency appears at zero angles. This is an indication that conical radiation and the zero-angle line of the ω_p branch have the same four-photon origin.

In our probing-field experiments, the field-intensity ratio was varied within broad limits, but the maximum signal due to the parametrically created wave of frequency $\omega'_\mu = 2\omega_L - \omega_\mu$ was obtained for a single ratio. The minimum intensity ratio for which the maximum in the region of the scattering branch could be recorded was 1:20.

We have also carried out a detailed study of scattering near the $3S_{1/2} - 3P_{1/2}$ resonant transition¹³ and have shown that the observed conical radiation near this transition is also due to the four-photon resonant parametric scattering process with partial spatial phase matching. However, the $3S_{1/2} - 3P_{1/2}$ transition has the specific feature that the redistribution of the $3S_{1/2}$ and $3P_{3/2}$ populations accompanying the emission of the three-photon line ($\omega_{3\text{ph}}^{3/2} = 2\omega_L - \omega_{3/2}$) has a substantial effect on the conical scattering angle.

6. CONCLUSION

Let us now summarize our results. Conical radiation, whose origin gave rise to extensive discussion in the literature, appears as a branch of the frequency-angular scattering diagram in a resonant medium. Conical radiation is due to the four-photon parametric scattering of a light beam of small cross section when the direction of propagation of the exciting radiation and of the three-photon line are the same. It is well-known that these factors ensure that the four-photon interaction occurs under spatial phase-matching with respect to the longitudinal coordinate alone, so that the frequency-angular diagram of the scattered radiation is asymmetric in frequency.

The basis for this interpretation is as follows. The shape of the scattering branch is described by the relationship between the refractive indices at the frequencies of the interacting waves (7), which follows from the phase-matching conditions (2). The experimental and calculated frequency-

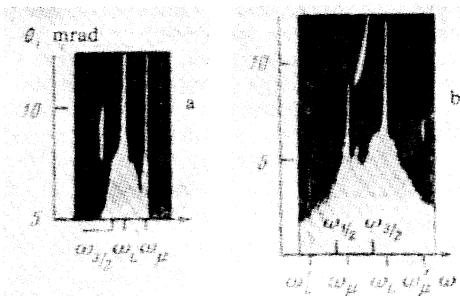


FIG. 5. Spectrogram recorded under bichromatic excitation: a— $\Omega_{3/2} = 6.6 \text{ cm}^{-1}$, $N = 10^{14} \text{ cm}^{-3}$, $P_L:P_\mu = 4:1$, $\omega_\mu - \omega_L = 11.2 \text{ cm}^{-1}$, b— $\Omega_{3/2} = 8.2 \text{ cm}^{-1}$, $N = 2.7 \cdot 10^{14} \text{ cm}^{-3}$, $P_L:P_\mu = 4:1$, $\omega_\mu - \omega_L = 22.4 \text{ cm}^{-1}$.

angular diagrams were found to agree in a broad range of laser frequency and sodium-vapor concentration. This includes values of the conical radiation angle and the position of the zero-angle line. A correlation has been found between the onset of conical radiation and small-scale self-focusing. It was demonstrated experimentally that radiation of frequency ω_p originated in regions with small lateral dimensions. The probing-field method can be used to perform a direct verification of whether the conical radiation is due to the four-photon resonant parametric scattering process. Probing-field experiments do, in fact, confirm our interpretation.

Let us now consider some of the results obtained by other workers. We have examined the data published in Refs. 1 and 4–6 and have concluded that these experimental data are in good agreement with our model of the origin of conical radiation.

Thus, in the latter experiments, conical radiation was emitted only for positive detuning of the strong-field frequency from resonance and under the condition of self-focusing. There was also a linear relationship between θ^2 and N , and an inversely proportional relationship between θ^2 and detuning. Figure 4 of Ref. 4, which reports on conical radiation in barium vapor, shows the conical scattering angle θ as a function of the detuning of the laser field. We have used our formula (9) to analyze these measurements and have found good agreement for $K = 1.46$, which agrees with our hypothesis.

The experimental results reported in Refs. 5 and 6 on conical radiation near the $3S_{1/2}-3P_{1/2}$ transition in sodium vapor can be well approximated by (9) with $K = 1.41$, which is in excellent agreement with our model. It is important to note that, according to the model considered in Refs. 5 and 6, four-photon mixing occurs in the self-focused laser beam when the phase-matching conditions are satisfied for plane

waves (1) and the emission of the high-frequency ω_3 band can be trapped within the filament as a result of total internal reflection. For radiation of frequency ω_3 , the refractive index outside the filament is greater than inside, so that the angle $\theta(\omega_p)$ to the axis is greater than the value predicted by (9) with $K = 1.41$ for refraction at the lateral boundary. However, our probing-field experiments have shown that conical radiation can also be produced at the frequency ω_3 when the probing-field frequency ω_μ is tuned in the ω_p region (Fig. 4b), i.e., when the refractive index outside the filament is less than inside. These experimental facts are therefore inconsistent with the model considered in Refs. 5 and 6.

¹The lower portions of the diagram, which are symmetric to the upper portions, are not shown.

¹S. H. Skinner, *Opt. Commun.* **41**, 255 (1982).

²Yu. M. Kirin, S. G. Rautian, A. E. Semenov, and B. M. Chernobrod, *Pis'ma Zh. Eksp. Teor. Fiz.* **11**, 340 (1970) [*JETP Lett.* **11**, 226 (1970)].

³A. I. Plekhanov, S. G. Rautian, V. P. Safonov, and B. M. Chernobrod, *Pis'ma Zh. Eksp. Teor. Fiz.* **36**, 232 (1982) [*JETP Lett.* **36**, 284 (1982)].

⁴C. H. Skinner and P. D. Kleiber, *Phys. Rev. A* **21**, 151 (1980).

⁵D. J. Harter and R. W. Boyd, *Opt. Lett.* **7**, 491 (1982).

⁶D. J. Harter and R. W. Boyd, *Phys. Rev. A* **29**, 739 (1984).

⁷V. N. Lugovoi and I. I. Sobel'man, *Zh. Eksp. Teor. Fiz.* **58**, 1283 (1970) [*Sov. Phys. JETP* **31**, 690 (1970)].

⁸V. N. Lugovoi and A. M. Prokhorov, *Zh. Eksp. Teor. Fiz.* **69**, 84 (1975) [*Sov. Phys. JETP* **42**, 42 (1975)].

⁹G. V. Venkin, D. N. Klyshko, and L. L. Kulyuk, *Kvantovaya Elektron. (Moscow)* **4**, 982 (1977) [*Sov. J. Quantum Electron.* **7**, 550 (1977)].

¹⁰G. C. Bjorklund, *IEEE J. Quantum Electron.* **QE-11**, 287 (1975).

¹¹V. N. Lugovoi and A. S. M. Prokhorov, *Usp. Fiz. Nauk* **111**, 203 (1973) [*Sov. Phys. Usp.* **16**, 658 (1971)].

¹²V. N. Bel'tyugov, V. I. Nalivaiko, A. I. Plekhanov, and V. P. Safonov, *Kvantovaya Elektron. (Moscow)* **8**, 1382 (1981) [*Sov. J. Quantum Electron.* **11**, 837 (1981)].

¹³A. I. Plekhanov, S. G. Rautian, V. P. Safonov, and B. M. Chernobrod, Preprint No. 231, Institute of Automation and Electrometry, Siberian Division, Academy of Sciences of the USSR, Novosibirsk, 1984.

Translated by S. Chomet